NIGERIAN JOURNAL OF HYDROLOGICAL SCIENCES

Vol. 4 2016 ISSN: 2315-6686

Published by:

NIGERIA ASSOCIATION OF HYDROLOGICAL SCIENCES

Application of Geosciences Techniques for the Assessment of Dumpsite Leachates and Groundwater Pollution in Regolith Aquifers

C.I. Unuevho[1], M. Ancho[1], A.N. Amadi[1], K.M. Onuoha[2] and M. Ogunbajo[1]
[1]Department of Geology, Federal University of Technology, Minna, Nigeria.
[2]Department of Geology, University of Nigeria, Nsukka, Nigeria.
*Corresponding author: unuevho@gmail.com

Abstract

Groundwater in regolith aquifer around Awan-Nepa dumpsite in Keffi (north-central Nigeria) was assessed for contamination attributable to heavy metal leachates. The assessment was conducted by mapping elevation of static water table, geo-elecrtic sounding, determining concentrations of heavy metal ions in filtrate created using the dumpsite soil colloid, and in water samples obtained from twenty wells dug manually into the regolith within the dumpsite vicinity. Contamination extent was evaluated using contamination factor (CF), index of pollution load (PLI), index of metal pollution (MPI), and index of geo-accumulation (I_{geo}). Groundwater convergence zones were revealed at 2.5Km SW and 4Km NW of the dumpsite. Topsoil at the dumpsite was found to be thin (0.8-1m) and characterised with moderateresistivity (140-240Ωm) and transverse unit resistance (120-150 Ωm^2). These values indicate high permeability and hydraulic conductivity within the topsoil. Low resistivity (35-45 Ωm) characterised the regolith at the dumpsite, indicating the presence of a contaminant plume. Surface runoff from rainfall dissolved some metal components of the dumpsite waste. Part of the dissolved metals infiltrated the regolith, and built up a contaminant plume. Concentrations of arsenic, chromium, manganese, nickel and lead is higher than 0.7 mg/l in water samples obtained from the regolith wells. This concentration value exceeds World Health Organisation prescribed limit for potable water. Values of CF indicate moderate level contamination from arsenic and moderate to very high contamination level from cadmium and copper at the dumpsite. Less than 0.024 PLI value reveals that the area is free from heavy metals aggregate effects. Approximately 0.6 MPI value shows the dumpsite's vicinity is free from anthropogenic pollution attributable to heavy metals, in spite of some contamination at the dumpsite. The spatial concentration maps reveal a contamination plume at the dumpsite, and a gradual attenuation in contamination level outward from the dumpsite. The maps also show that the concentration of barium, chromium, arsenic and lead within the convergence is lower than 5% of the concentration in filtrate from the dumpsite's soil colloid. Water in the groundwater convergence zones is fit for drinking.

Keywords: Regolith aquifer, permeability, Hydraulic conductivity, Dumpsite, Groundwater convergence

Introduction

Common diseases within the environs of such dumpsites include hypertension, skin cancer, kidney failure, liver dysfunction, osteomalacia, osteoporosis, deafness and neurological diseases. Such diseases have been associated with ingestion of heavy metals (Deming, 2002; Adegoke *et al.*, 2009; Ayolabi *et al.*, 2013; Singh *et al.*, 2015). It is this association that necessitates the assessment of groundwater contamination that is connected with heavy metals leached into the regolith aquifer in the environs of Agwa-Nepa dumpsite. Low electrical resistivity values generated from geo-electrical sounding are traditionally employed to identify areas with unusually high amount of ions related to groundwater contaminant plumes (MacFarlane *et al.*, 1983; Becker, 2002; Rosquit *et al.*, 2003; Jegede *et al.*, 2011; Carpenter and Reddy, 2011; Omolayo and Tope, 2014).The issue with the approach is that highly clayey interval within the regolith could simulate similar low resistivity values and misguide interpretation. Pollution status is also sometimes qualitatively categorised using concentration of ions obtained from chemical analysis of samples of groundwater (Adegoke *et al.*2009; Alile *et al.*, 2013; Ayolabi *et al.*, 2013; Omolayo *et al.*, 2014). Such qualitative categories could be subjective, blurred and do fail to quantitatively specify contamination extent. Besides this, few published works exist on the use of numerical indices developed from geo-electric resistivity measurements to ascertain transportation direction of contaminant ions from dumpsites into groundwater contained in regolith. This work deploys numerical indices such as CF, PLI, MPI, and I_{geo} to evaluate ionic concentrations of heavy metals determined in groundwater by Inductively Coupled Plasma- Mass Spectrometry (ICP-MS) method of chemical analysis. Furthermore, the work strives to infer migration direction of contaminant ions from dumpsite leachate into groundwater from hydraulic conductivity criteria developed from geo-electrical resistivity data.

Methodology

Agwan-Nepa dumpsite is located in Keffi, north-central Nigeria, within Latitudes 8°49'00"N, 8°53'00"N and Longitudes 7°51'00"E, 7°55'00"E (Fig.1). The dumpsite is massive and many inhabitants within its environs drink water fetched from hand-dug wells tapping its regolith aquifer.

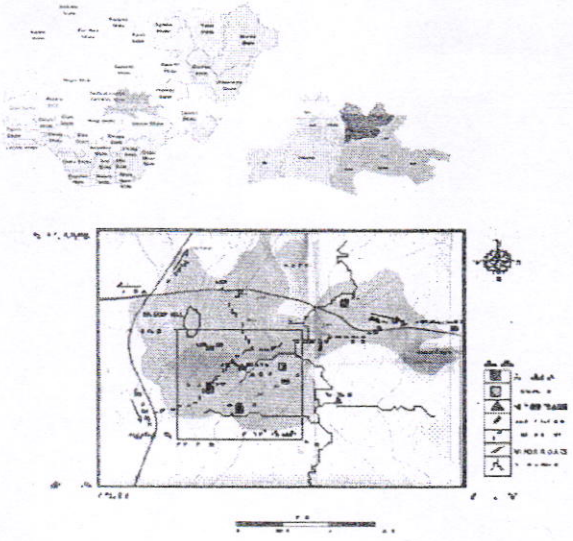

Fig.1: Location map of Agwan-Nepa dumpsite

Detailed lithological mapping of the area was carried out. Static water table elevation was determined by subtracting depth to static water table from the elevation of the top of each well's concrete protection, obtained using a Geographic Positioning System(GPS) device. Soil sample was taken from depth of 0.8m at the dumpsite because exposed geological sections in the area revealed that the soil thickness is generally less than 1.0m. The sample was soaked in a clean plastic bottle containing one litre of distilled water and the resulting colloid was shaken vigorously and left to settle for one week. This was then filtered and the filtrate labelled L0. Water table elevation map was generated with Suffer 11 contouring software. Samples of groundwater were taken from twenty wells dug manually into the regolith (locally called hand-dug wells). These samples were labelled L1-L20. Ionic concentrations of heavy metals comprising arsenic (As), barium (Ba), cadmium (Cd), chromium (Cr), copper (Cu), iron (Fe), manganese (Mn), nickel (Ni), and zinc (Zn) were determined in the twenty groundwater samples (L1 to L20) and filtrate (L0) using ICP-MS method, at Acme Laboratory in Vancouver BC, Canada. The laboratory was chosen for the analysis because it employs state-of-the-art equipment and software for generating chemical data with accuracy level required for making inferences concerning human health. Maps illustrating the spatial variations of each heavy metal's concentration were produced using Suffer 11. The method of Tijani *et al.*(2004), Sarala *et al.*(2013), Singh *et al.*(2013), and Onwuka *et al.* (2014) was used to calculate CF.

$$CF = \frac{C_S}{B_n} \quad (1)$$

In Equation 1, C_s represents the measured concentration of each heavy metal in a sample, and B_n is the average crustal abundance of the corresponding metal (obtained from Mason, 1966). Calculation of PLI was carried out using the method of Sarala and Uma (2013), and Onwuka *et al.* (2014):

$$PLI = (CF_1 \times CF_2 \times CF_3 \times CF_4 \times \ldots\ldots CF_{n-1} \times CF_n)^{1/n} \quad (2)$$

In Equation 2, CF_i represents each heavy metal's Contamination Factor in a sample while 'n' represents the whole number of heavy metals utilised in the computation for each sample. Sarala and Uma (2013) method was employed to calculate MPI:

$$MPI = \text{Log}\Sigma_{n=1}^{10} \left(\frac{X}{B_n}\right) \quad (3)$$

'X' in Equation 3 represents average concentration value for each metal in all regolith groundwater sample and B_n represents a standardiser, which is of each corresponding metal's average crustal concentration.

Calculated of I_{geo} was made with the method of Sarala *et al.* (2013) and Onwuka *et al.* (2014):

$$I_{geo} = \text{Log}_2 \frac{C_n}{1.5B_n} \quad (4)$$

where the concentration of each metal in a sample is represented by C_n while the mean crustal abundance for the corresponding metal is represented by B_n (obtained from Manson, 1966). Table 1 was employed in categorising the groundwater contamination status: after Hakanson, (1980); Sarala *et al.* (2013) and Singh *et al.* (2014).

Table 1: Contamination factor (Cf) and Geoaccumulation Index (Igeo) categorisation

CF/Igeo	Category
<1	Neglible contamination factor
1-3	Mild contamination factor
3-6	Substantial contamination factor
>6	Very high contamination factor

Contamination is implied when PLI or MPI or Igeo is greater than 1, while values lower than 1 indicates a clean status (Sarala *et al.*, 2013). Vertical Electrical Sounding (VES) was carried out at twenty locations, using the Schlumberger field geometry in which maximum electrode spacing (AB) was 100m. Such electrode spacing guarantees that the electrical current generated from an external source (a battery) would investigate the entire regolith interval. Values of apparent resistivity (ρ_a) were calculated using Unuevho *et al.* (2012)

$$\rho_a = \left(\frac{(AB)^2 - (MN)^2}{MN}\right)\frac{\pi}{4}\frac{\Delta V}{I} \qquad (5)$$

where 'AB' and 'MN' are respectively current electrodes spacing and potential electrodes spacing, V is the potential difference between the potential electrodes and I is the current passing between the current electrodes. Win Resist interpretation software was used to generate geoelectric sections from the apparent resistivity data.

Longitudinal unit conductance (S) and transverse unit resistance (T) values were obtained for topsoil and weathered basement intervals, using the methods of Mailet (1974):

$$S = \sum_{i-1}^{n} \frac{h_i}{\rho_i} \qquad (6)$$

$$T = \sum_{i-1}^{n} h_i \rho_i \qquad (7)$$

The thickness and true resistivity value of each unit in a geoelectric section are represented respectively by h_i and ρ_i in Equations 6 and 7. Maps representing areal values of S, T and true resistivity ρ were created using Surfer 11 contouring software. Elevation data on static water table was integrated with ionic concentration data for heavy metals, as well as S, T and resistivity data. The integrated data was used to validate the presence of leachate contaminant plume at the dumpsite, to decipher the plume movement direction, as well as to ascertain the status of contamination of groundwater within the regolith.

Results and Discussion

Flow pattern and its implication

Static water table elevation map (Fig.2) revealed a groundwater divide that trends NNW-SSE. The divide terminates about 0.7Km SE of Karoffi. The groundwater flow direction is NNE and SSW northwards and southwards of the divide respectively. The position of the dumpsite on the SE of the divide, and the opposing groundwater flow directions on either side of the divide creates a geomorphologic setting that protects groundwater on the north of the divide from the dumpsite leachates. Converging groundwater flow system at 2.5Km SW of the dumpsite suggests that distant areas beyond the convergence zone are free from influence of the dumpsite leachate. Another groundwater convergence zone exists at about 1Km SW of Karoffi, which is about 4Km NW of the dumpsite. This indicates that groundwater flow system from the dumpsite does not extend beyond 4Km NW of the dumpsite. The rapid change in static water table elevation, east of Sabon Lavi (around L13) and around south of Karoffi (around L16) implies poor hydraulic conductivity, low permeability and transmissivity of regolith (combined topsoil and weathered layers) in these places. Apart from the vicinities of L13 and L6, static water table elevation changes slowly.

The resistivity sounding data revealed that H-type geo-electrical resistivity curve dominantly characterise the study area (Fig.3). This indicates three geo-electric layers: top soil, weathered basement and fresh basement.The top soil is very thin (0.8-1m) at the dumpsite and its immediate vicinity (Fig.4). The weathered basement is slightly thin (4.5-6.5m) around the dumpsite (Fig.5).Moderate resistivity values (140-240Ωm) and transverse unit resistance (T) values (120-150 Ωm^2) indicate high permeability and hydraulic conductivity within the top soil at the dumpsite (Figs.6 and 7 respectively).Figure 8 reveals that the weathered basement's T value is moderate to high (150-350 Ωm^2) within the dumpsite vicinity. The T value is very high (750-1250 Ωm^2) in the southern areas and high in the central portions (350-550 Ωm^2). The weathered basement's S value (Fig.9) is low (0.06-0.19Ω) at the dumpsite, and moderate (0.19-0.29Ω) in the central portion and the on the SW of the dumpsite.

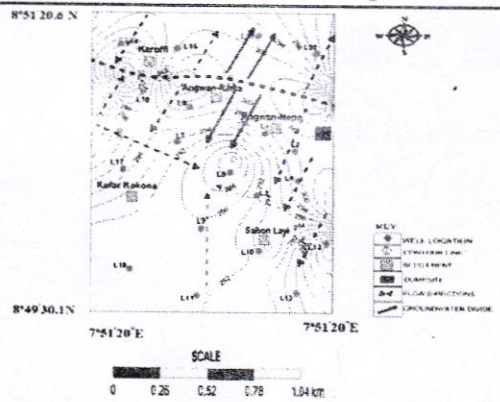

Fig. 2: Static water table elevation Contour map of Angwan-Nepa dumpsite and its environs

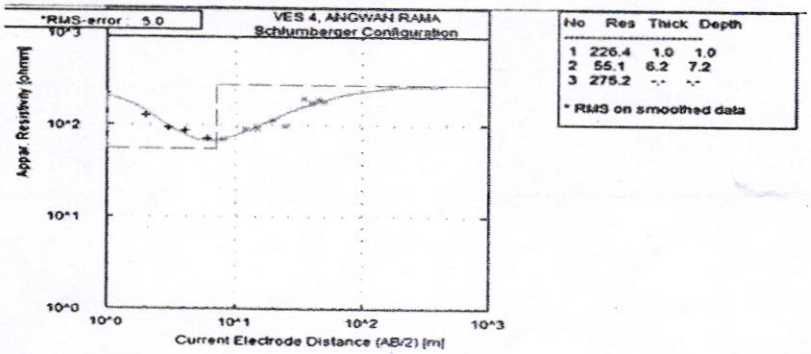

Fig.3: Representative H-type curve for Agwan-Nepa

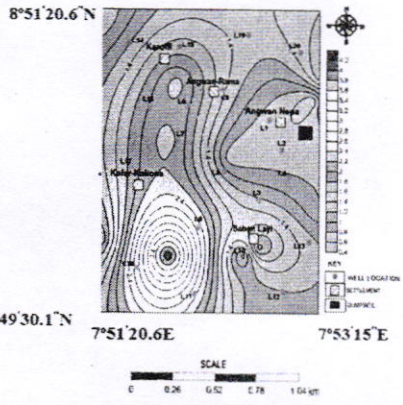

Fig.4: Topsoil thickness map

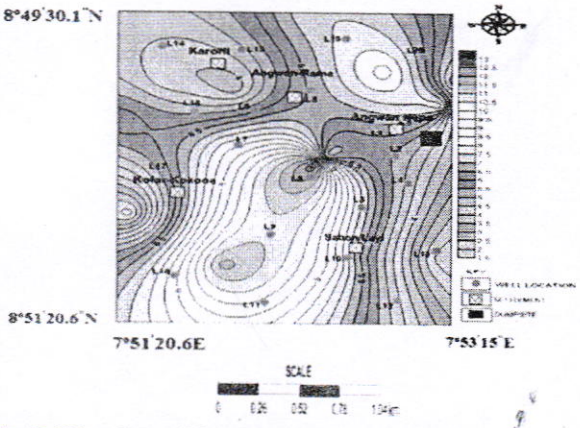

Fig.5: Weathered basement thickness map

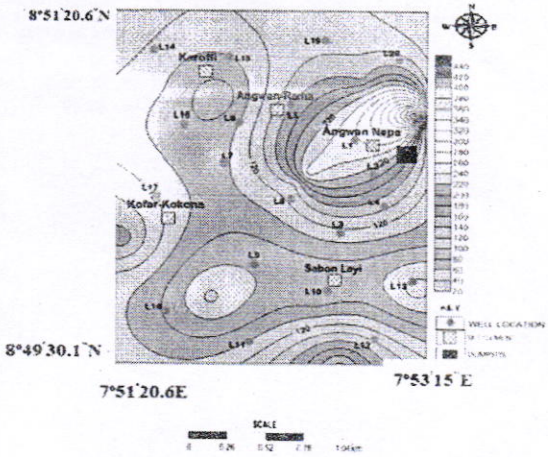

Fig.6: Topsoil's isoresistivity map

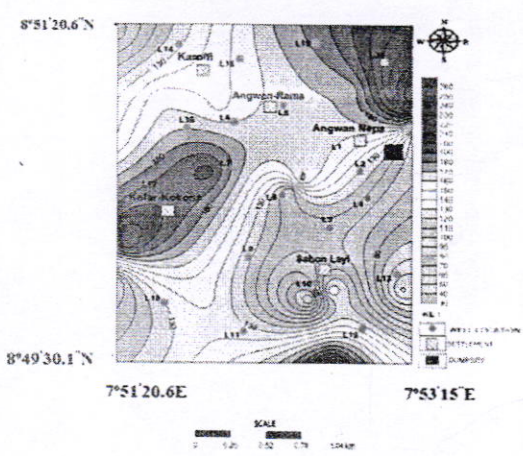

Fig.7: Topsoil's T map

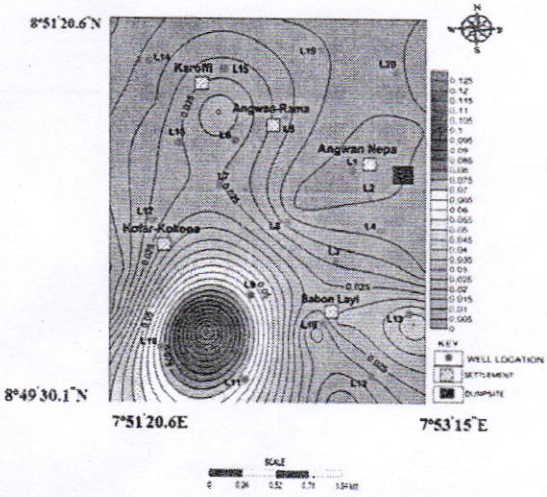

Fig.8: Weathered basement's T map

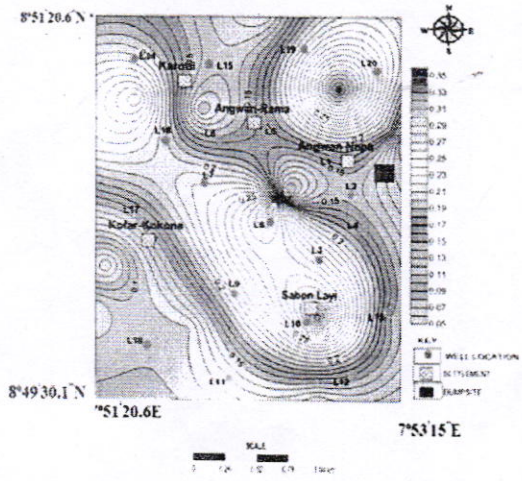

Fig.9: Weathered basement's S map

The pattern of T and S values, as well as slowly changing static water table elevation, indicates widespread high permeability and hydraulic conductivity in the area. Weathered basement isoresistivity map (Fig.10) reveals lowest resistivity values (10-15 Ωm) on east of Sabon Layi. This reflects high clay content already indicated by rapid changes in water table elevation in

the area. The map also reveals very low resistivity values (35-45Ωm) at the dumpsite. This suggests the presence of a contaminant plume associated with groundwater at the dumpsite. Slightly acidic rain water falling upon the miscellaneous waste at the dumpsite possesses capacity to dissolve some portion of the metal components in the waste. The dissolved metals would travel in percolating solution through the thin soil interval into the weathered basement, where it is intercepted by groundwater within the regolith, and then gradually build up a contaminant plume.

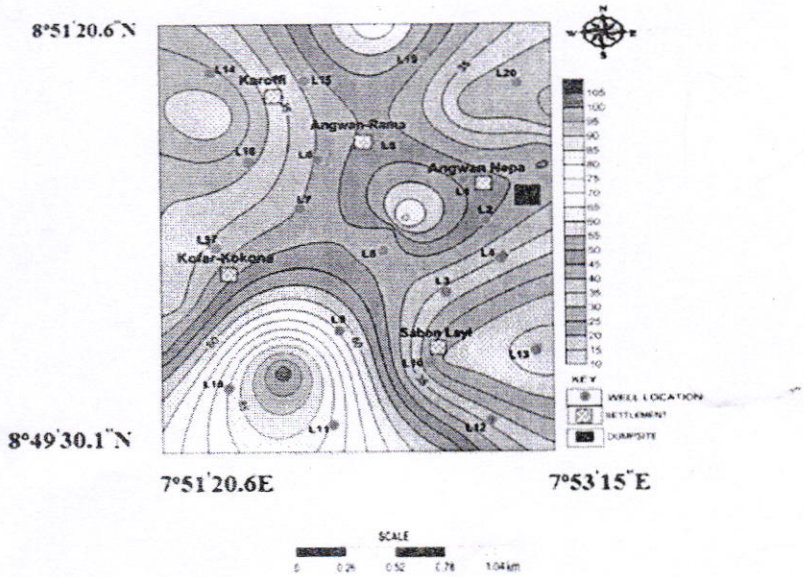

Fig.10: Weathered basement's isoresistivity map

Heavy metal concentration and its spatial distribution

Concentration of each heavy metal in the filtrate from dumpsite's soil sample colloid (L0) and water samples from the hand-dug wells is given in Tables 2 and 3. Mean concentration of As, Ba, Cd, Cr and Cu is respectively 0.29, 0.32, 0.27, 0.41and 2.22 mg/l. Their respective range is 0.05 – 0.8, 0.02 – 0.7, 0.05 – 0.66, 0.17 – 0.75 and 0.1 – 5.4 mg/l. Fe, Mn, Ni, Pb and Zn have respective average concentrations of 1.25, 0.76, 0.81, 0.34, and 2.63 mg/l. Their respective concentration range is 0.3 -6.9, 0.05 – 1.65, 0.21 – 0.18, 0.01 – 1.04 and 0.5 – 5.7 mg/l. The graphical illustration of each of the metal's mean concentration in comparison with WHO (2011) prescribed standard for potable water is given in Fig.11. The mean concentration of each of these metals (with the exception of Zn) exceeds the maximum limit prescribed by

WHO (2011) for potable water. This is because higher concentration of zinc is required by the human body for metabolic functions. This is the reason why medical practitioners commonly prescribe zinc to be taken as a dietary supplement to body metabolic patients.

Table 2: Concentration of each heavy metal in filtrate from dumpsite soil's colloid (L0) and water samples from hand-dug wells (L1-L10)

Sample No.	Parameter (mg/l)									
	As	Ba	Cd	Cr	Cu	Fe	Mn	Ni	Pb	Zn
L0	**3.0**	**5.8**	**0.7**	**3.0**	**8.0**	**10**	**5.5**	**3.0**	**4.0**	**30**
L1	0.12	0.02	0.40	0.36	1.70	1.1	0.40	1.38	0.14	3.14
L2	0.12	0.04	0.20	0.26	4.90	0.6	0.20	0.47	0.88	1.30
L3	0.80	0.09	0.16	0.22	2.80	0.4	0.20	0.38	0.78	3.25
L4	0.18	0.4	0.51	0.31	1.53	0.9	0.50	1.08	0.11	5.67
L5	0.25	0.3	0.19	0.33	1.03	0.5	0.60	0.39	0.75	1.89
L6	0.11	0.3	0.18	0.34	4.30	0.7	0.20	0.43	0.76	1.55
L7	0.10	0.2	0.25	0.34	2.76	0.4	0.07	0.58	0.72	2.38
L8	0.05	0.2	0.17	0.36	1.24	0.9	0.09	1.50	0.82	2.12
L9	0.12	0.2	0.51	0.17	5.41	0.3	1.41	0.43	0.56	2.10
L10	0.23	0.3	0.38	0.35	1.72	0.6	0.12	0.56	1.04	2.43

Table 3: Heavy metals' concentration in water samples from hand-dug wells (L11-L20), heavy metals' concentration range and mean concentration

Sample No.	Parameter (mg/l)									
	As	Ba	Cd	Cr	Cu	Fe	Mn	Ni	Pb	Zn
L11	0.10	0.3	0.21	0.39	1.90	0.52	0.30	0.50	0.10	3.67
L12	0.12	0.2	0.66	0.75	2.59	1.96	0.51	1.29	0.22	5.70
L13	0.52	0.6	0.37	0.32	1.24	3.2	1.65	0.68	0.87	3.68
L14	0.21	0.3	0.59	0.44	3.40	6.9	0.61	1.17	0.86	2.16
L15	0.35	0.4	0.10	0.75	0.80	1.0	0.98	0.80	0.10	0.50
L16	0.21	0.4	0.10	0.62	0.70	1.0	0.23	0.70	0.30	1.80
L17	0.32	0.4	0.10	0.72	0.20	1.0	0.80	0.55	0.10	1.10
L18	0.50	0.5	0.10	0.23	0.10	1.0	0.05	1.80	0.10	3.30
L19	0.80	0.7	0.33	0.52	4.90	1.0	0.51	0.21	0.10	2.30
L20	0.60	0.51	0.18	0.34	1.09	0.95	1.37	0.92	0.74	1.57
Mean	0.29	0.32	0.27	0.41	2.22	1.25	0.76	0.81	0.34	2.65
Range	0.05-0.8	0.02-0.7	0.05-0.66	0.17-0.75	0.1-4.9	0.3-6.9	0.05-1.65	0.21-1.8	0.10-1.04	0.5-5.7
WHO	0.01	0.7	0.003	0.05	2	-	0.4	0.02	0.01	3
NIS	0.01	0.7	0.003	0.05	1	0.3	0.2	0.02	0.01	3

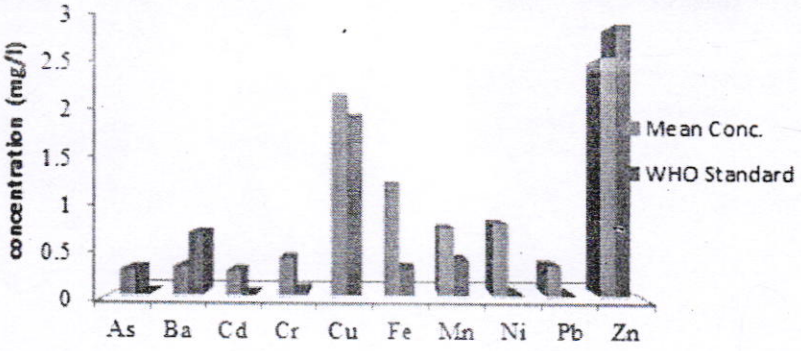

Fig.11: Each heavy metal's mean concentration vis-à-vis WHO prescribed limit for potable water

The concentration of As in all the samples is greater 0.01mg/l. The highest concentration of As occurs at the dumpsite, from where the concentration begins an approximately radial outward decrease (Fig.12). The lowest concentration of As exists within the zone where groundwater flow converges, at approximately 1Km south-westwards of the dumpsite.

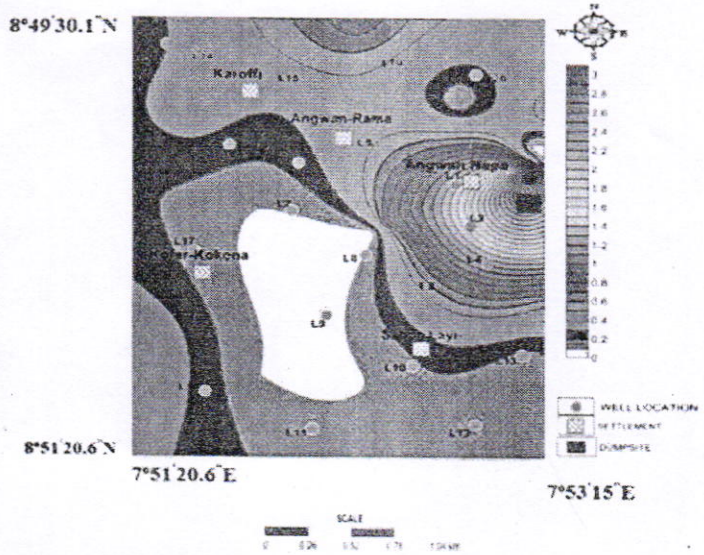

Fig. 12: Ionic concentration map for arsenic within Angwan-Nepa dumpsite and its vicinity

Spatial distribution of Cd concentration (Fig.13) follows the concentration pattern of As. However, a reversal occurs at about 0.5Km south of the dumpsite (on the NE of Sabon Layi) where a concentration syncline (or depression) exists. The concentration syncline is a probable geo-accumulation effect produced when regolith particles adsorb Cd ions from solution onto their surface, in response to decreasing regolith permeability and hydraulic conductivity. Solubility and concentration of Cd ions increased again southerly towards L3 due to improvement in regolith permeability along this direction.

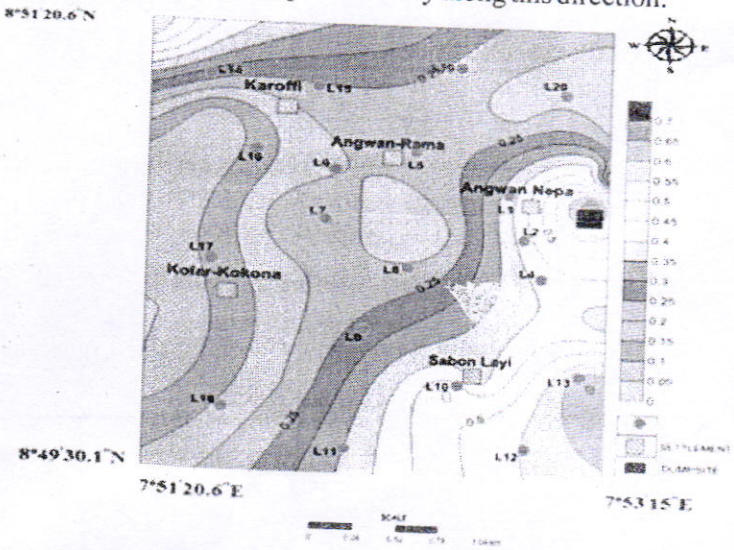

Fig. 13: Concentration map for cadmium within Angwan-Nepa dumpsite and its vicinity

Concentration of Cr ions in all the water samples is higher than the 0.05 mg/l healthy limit advised by WHO (2011). Concentration of Cr ions decreases in outward radial pattern from its plume at the dumpsite (Fig.14), in similarity with Cd. The absence of mafic and ultramafic rocks in the area indicates that the high concentration of Cr ions is attributable to the dumpsite leachate, and thus anthropogenic. The concentration of Ni exceeds the permissible limit of 0.02mg/l in all the samples. Highest Ni concentration occurs at the dumpsite and then the concentration decreases outward (Fig.15). Concentration reversal SW of Kofar Kokona is likely due to increased concentration arising from probable presence of nickel sulphide minerals within relict veins in the weathered schist in the area. On the other hand, the concentration of Pb exceeds the WHO (2011) prescribed limit of 0.01mg/l in all the water samples, with the concentration plume occurring at the dumpsite and decreasing outward from there (Fig.16).

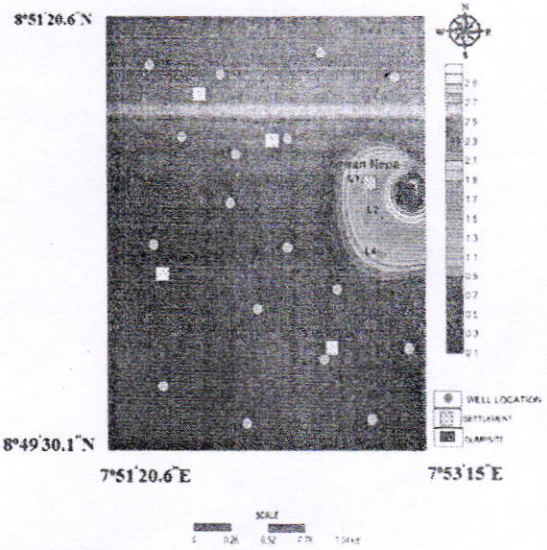

Fig. 14: Concentration map for chromium within Angwan-Nepa dumpsite and its vicinity

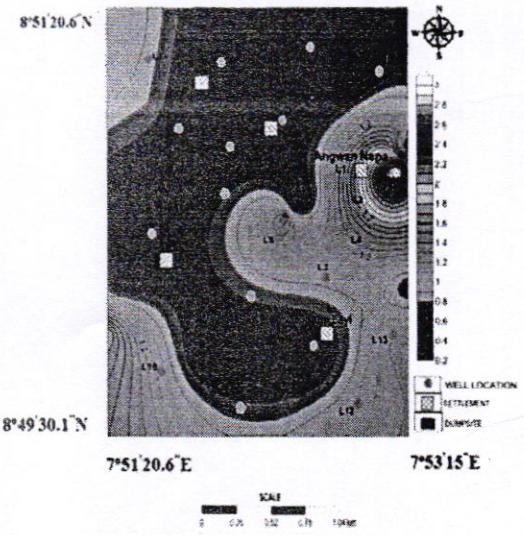

Fig. 15: Concentration map for nickel within Angwan-Nepa dumpsite and its vicinity

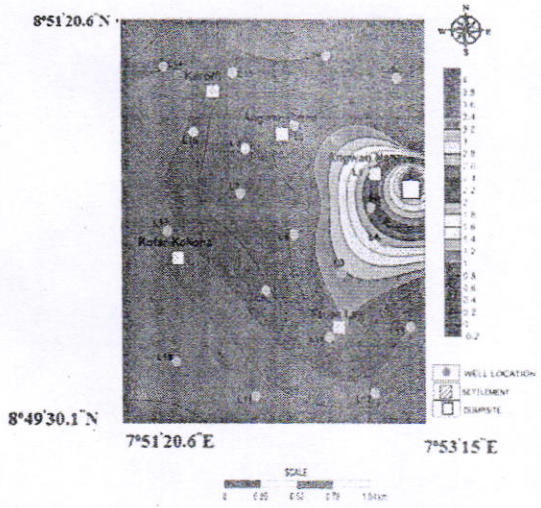

Fig. 16: Concentration for lead within Angwan-Nepa dumpsite and its vicinity

Concentration of Mn exceeds the WHO (2011) prescribed limit of 0.4mg/l in all the water samples. It is highest at the dumpsite, and then decreases south-westward and southward as a result of dilution associated with groundwater flow (Fig.17). The reversal in concentration trend on the SSE of Kofar Kokona is probably due to the presence of magnetite in relict mineralised veins within the weathered schist in this area.

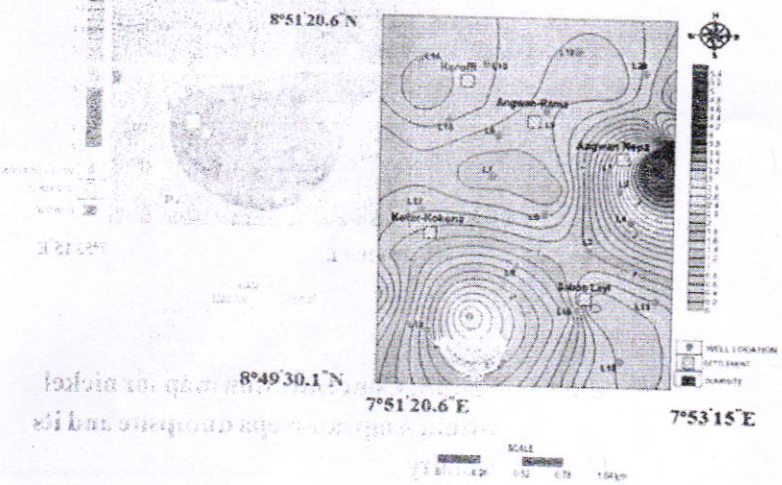

Fig. 17: Concentration map for manganese within Angwan-Nepa dumpsite and its vicinity

Spatial concentration map for Cu (Fig.18), Fe (Fig. 19), Zn (Fig.20) and Ba (Fig.21) all reveal a concentration plume at the dumpsite, and a radial outward concentration decrease due concentration attenuation related to dilution in direction of groundwater flow.

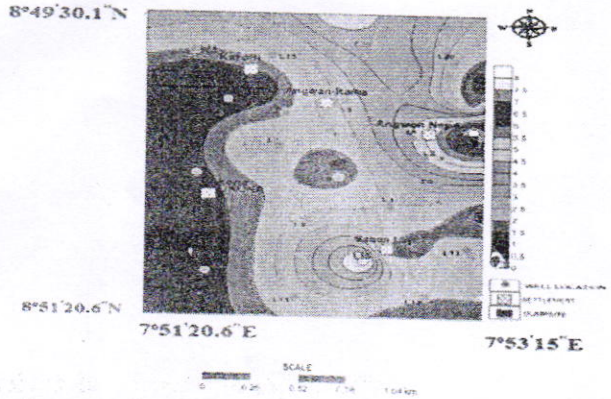

Fig. 18: Concentration map for copper within Angwan-Nepa and itsvicinity

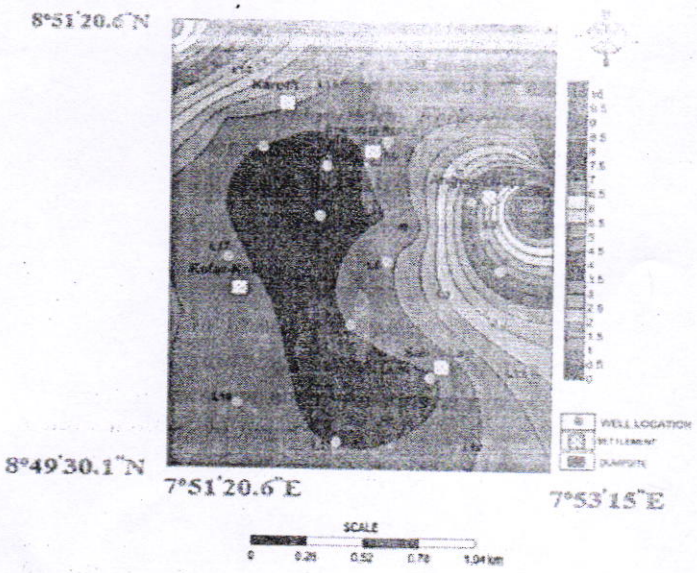

Fig. 19: Concentration map for iron within Angwan-Nepa dumpsite and its vicinit

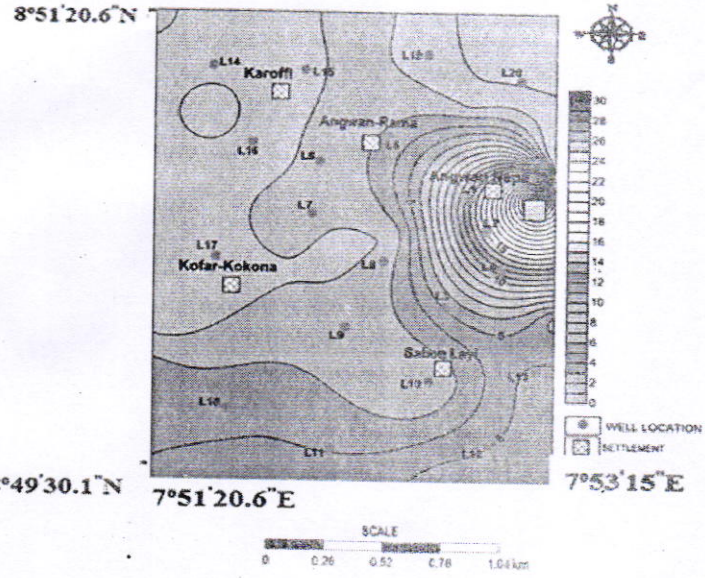

Fig. 20: Concentration map for zinc within Angwan-Nepa dumpsite and its vicinity

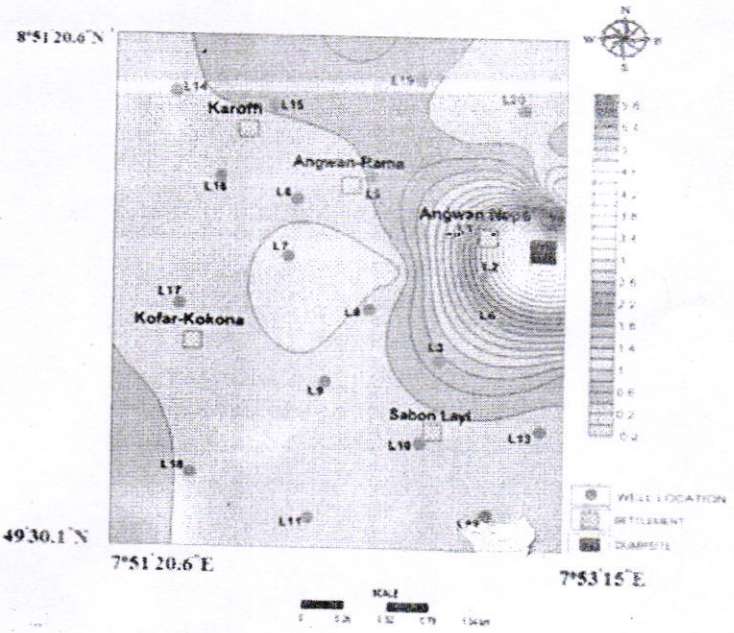

Fig.21: Concentration map for barium in Angwan-Nepa dumpsite and its vicinity

The computed contamination factor (CF) and pollution load index (PLI) for samples L0-L10 and L11 – L20 are given in Table 3. The mean concentration for each of the heavy metals in all the water samples and their average concentration in world rock (employed in the computations) are given in Table 4.

The CF for As reflects mild contamination level from As at the dumpsite (L0). The CF for Cd and Cu shows mild and very high contamination levels respectively at the dumpsite. The PLI value is less than 1.00 in the area and this implies that the overall contamination attributable to the aggregate effects of the heavy metals is negligible in the area. The computed metal pollution index (MPI) value for the area is given in Table 5. The MPI value is lower than 1.00 (approximately 0.6) and this indicates that the study area is yet to suffer anthropogenic pollution from heavy metals, though some contamination has occurred, especially at the dumpsite. I_{geo} value for each of the metals is given in Table 6. It reveals mild accumulation of As at the dumpsite. It also reveals geoaccumulation of Cd at the dumpsite and at L10, L12, L13, and L14.

Table 3: Computed CF and PLIof heavy metals in Angwan-Nepa dumpsite and its environs

Sampie No.	CF										PLI
	As	Ba	Cd	Cr	Cu	Fe	Mn	Ni	Pb	Zn	
L0	1.67	0.0014	3.50	0.30	8.00	0.0002	0.0058	0.04	0.21	0.43	0.098
L1	0.06	0.00005	2	0.004	0.031	0.00002	0.000042	0.018	0.011	0.05	0.004
L2	0.06	0.00009	1	0.003	0.089	0.00001	0.00021	0.006	0.068	0.02	0.006
L3	0.40	0.00021	0.80	0.002	0.050	0.00001	0.00022	0.005	0.06	0.05	0.007
L4	0.18	0.00094	2.55	0.003	0.028	0.00002	0.00052	0.003	0.0085	0.08	0.008
L5	0.10	0.00071	4.75	0.003	0.019	0.00001	0.00063	0.005	0.058	0.03	0.006
L6	0.06	0.00071	0.90	0.003	0.078	0.00001	0.00021	0.006	0.058	0.03	0.006
L7	0.05	0.00047	1.25	0.003	0.050	0.00001	0.000073	0.008	0.055	0.03	0.006
L8	0.03	0.00047	0.85	0.004	0.022	0.00002	0.000095	0.02	0.063	0.03	0.015
L9	0.06	0.00047	2.55	0.002	0.098	0.00001	0.0012	0.006	0.043	0.03	0.008
L10	0.13	0.00071	1.60	0.004	0.031	0.00001	0.00012	0.008	0.08	0.04	0.007
L11	0.05	0.00071	1.05	0.0039	0.035	0.000010	0.0032	0.0066	0.0076	0.052	0.0073
L12	0.06	0.00047	3.3	0.0075	0.047	1.000392	0.00053	0.0017	0.017	0.081	0.0230
L13	0.29	0.00014	1.85	0.0032	0.023	0.000064	0.0017	0.0091	0.066	0.052	0.0110
L14	0.21	0.00071	2.95	0.0044	0.062	0.000138	0.00064	0.016	0.065	0.030	0.0142
L15	0.21	0.00009	0.25	0.0075	0.015	0.000002	0.0010	0.011	0.0076	0.007	0.0038
L16	0.12	0.00009	0.25	0.0062	0.013	0.000002	0.00024	0.0093	0.0023	0.026	0.0030
L17	0.18	0.00009	0.25	0.0072	0.003	0.000002	0.00084	0.0073	0.00077	0.016	0.0026
L18	0.28	0.00012	0.25	0.0023	0.001	0.000002	0.000053	0.024	0.0076	0.047	0.0028
L19	0.44	0.00017	1.65	0.0052	0.089	0.000002	0.00054	0.0028	0.0076	0.033	0.0058
L20	0.33	0.0012	0.9	0.0034	0.019	0.000019	0.0014	0.012	0.057	0.022	0.0099

Table 4: Mean concentrations of Heavy metals in water samples and their World rock surface Average from Manson (1966)

Parameter (mg/l)	As	Ba	Cd	Cr	Cu	Fe	Mn	Ni	Pb	Zn
Mean Conc. (mg/l)	0.29	0.32	0.27	0.41	2.22	1.25	0.76	0.81	7.27	2.63
World Surface Rock Ave. (mg/l)	1.8	425	0.2	100	55	500000	950	75	13	70

Table 5: Calculated MPI for the study area

Metals	average concentration x	Reference value Ref	x/ref
As	0.29	0.01	0.0029
Ba	0.32	0.7	0.224
Cd	0.27	0.003	0.00081
Cr	0.41	0.05	0.021
Cu	2.22	1	2.22
Fe	1.25	0.3	0.375
Mn	0.76	0.2	0.152
Ni	0.81	0.02	0.016
Pb	7.27	0.01	0.073
Zn	2.63	3	0.89
		Σ	**3.97**
		MPI = log Σ	**0.598**

Table 6: Computed I_{geo} for the heavy metals in the study area

	Igeo									
	As	Ba	Cd	Cr	Cu	Fe	Mn	Ni	Pb	Zn
L0	0.15	- 10.10	1.23	- 8.38	- 3.38	- 12.91	- 8.00	- 5.21	- 2.29	- 1.81
L1	- 4.51	- 11.06	0.41	8.70	-5.77	- 19.35	- 15.61	- 6.38	- 7.14	- 5.06
L2	- 4.51	- 11.66	- 0.60	- 9.20	- 4.08	- 20.25	- 12.80	- 7.90	- 4.47	- 6.38
L3	- 1.76	10.06	- 0.92	- 9.38	- 4.92	- 17.40	- 12.80	- 8.20	- 4.64	- 5.01
L4	- 3.92	- 11.06	0.77	- 8.90	- 5.71	- 16.35	- 11.48	- 6.70	- 7.48	- 4.21
L5	- 3.43	10.63	- 0.67	- 8.83	- 6.38	- 17.21	- 11.22	- 8.16	- 4.72	- 5.80
L6	- 4.64	- 11.06	- 0.74	- 8.76	- 4.27	- 16.71	-12.80	-8.04	- 4.68	- 6.06
L7	- 4.76	- 11.66	- 4.92	- 8.76	- 4.92	- 17.53	- 14.32	- 7.59	- 4.76	- 5.44
L8	- 5.72	- 11.66	- 0.84	- 8.70	- 6.06	- 16.35	- 13.94	- 6.27	- 4.57	- 5.64
L9	- 4.51	- 11.66	- 0.77	- 9.83	- 3.92	- 17.93	-10.10	- 8.38	- 5.11	- 5.64
L10	- 3.56	- 11.06	0.34	- 8.76	- 5.57	- 16.93	- 13.54	- 7.67	- 4.24	- 5.44
L11	- 4.51	- 11.06	- 0.51	- 8.59	- 5.44	- 17.14	- 8.83	- 7.83	- 7.62	- 4.84
L12	- 4.51	- 11.66	1.14	- 7.64	-5.01	- 15.23	- 11.44	- 6.51	- 6.51	-4.21
L13	- 1.76	- 10.06	0.30	- 8.90	- 6.06	- 14.51	- 9.71	- 7.38	- 4.47	- 4.84
L14	- 3.92	- 11. 06	1	- 8.43	- 4.61	- 13.41	- 11.18	- 6.64	- 4.47	- 5.57
L15	- 3.44	- 10.63	- 2.56	- 7.64	- 6.70	- 16.23	- 10.68	- 7.14	- 7.61	- 7.70
L16	- 4.64	- 10.63	- 2.56	- 7.93	- 6.88	- 16.23	-12.61	- 7.33	- 6.06	- 5.88
L17	- 4.76	- 10.63	- 2.56	- 7.70	- 8.70	- 16.23	- 10.80	-7.70	- 10.94	- 6.74
L18	- 9.04	- 10.32	- 2.56	- 9.38	- 9.70	- 16.23	-14.80	- 5.97	- 10.94	-5.01
L19	- 4.51	- 9.83	- 2.56	- 8.16	- 4.86	- 16.23	- 11.43	- 9.12	- 10.94	- 5.51
L20	- 5.56	- 10.51	- 0.74	-8.76	- 6.77	- 16.23	- 10.93	- 6.93	- 4.76	- 6.06

Conclusion

A groundwater divide that trends NNW-SSE was established in the northern vicinity of Agwan-Nepa dumpsite from static water table elevation data. The data revealed that groundwater flows north-northeast wards in the northern sector of the divide, and south-southwest wards on its southern region. The data also revealed a groundwater convergence zone within 2.5 Km SW and another convergence zone within 4 Km NW of the dumpsite. Hydro-geochemical data indicated that the groundwater flowing south-southwest wards of the divide contains dissolved As, Cd, Cr, Mn, Ni and Pb in toxic level concentrations on the WHO standard for potable water. Dilution at the groundwater convergence zones keeps the concentration of the dissolved metals within the WHO prescribed concentration range for potable water. The groundwater divide protects groundwater on its northern portion from the dumpsite leachates, and this keeps the groundwater there potable. Contamination indices data established moderate to very high level contamination of Cd, and Cu, and moderate level contamination of As at the dumpsite.

References

Adegoke, J. A., Agbaje, W. B. and Isaac, O. O. (2009). Evaluation of Heavy Metal Status of Water and Soil at Ikogosi Warm Spring, Ondo State Nigeria. *Ethiopian Journal of Environmental Studies and Management*, *2*(3): 88-93.

Alile, O. M., Ojuh, D. O., Iyoha, A. and Egereonu, J. C. (2011). Geoelectrical, DC. American Public Health Association, American Water Works Association and Water Environment Federation.investigation and hydrochemical analysis of groundwater in a waste dump environment, Isolo, Lagos. *African Journal of Environmental Science and Technology*, *5*(10): 795-806.

Ayolabi, E. A., Folorunso, A. F. and Kayode, O. T. (2013).Integrated Geophysical and Geochemical Methods for Environmental Assessment of Municipal Dumpsite System. *International Journal of Geosciences*, *4*(5): 850-862.

Becker, C. J. (2002). *Hydrogeology and leachate plume delineation at a closed municipal landfill, Norman, Oklahoma*. US Department of the Interior, US Geological Survey, p23-30.

Carpenter, P. and Reddy, K. (2011). Refuse conductivity variations following leachates injection in a bic reactive landfill cell: Modelling EM results and comparism with well logs. In *24th EEGS symposium on the Application of Geophysics to Engineering and Environmental problems.*

Deming, D. (2002). *Introduction to hydrogeology*.McGraw-Hill College, p468.

Hakanson, L. (1980). Ecological Risk Index for Aquatic Pollution Control: A Sedimentological Approach. *Water Research*, 14(975), 1001.

MacFarlane, D. S., Cherry, J. A., Gillham, R. W. and Sudicky, E. A. (1983). Migration of contaminants in groundwater at a landfill: A case study: 1. Groundwater flow and plume delineation. *Journal of Hydrology*, *63*(1): 1-29.

Maillet R. (1947). The fundamental equations of electrical prospecting.*Geophysics* 12(4): 551-556

Manson, B. (1966). Principles of geochemistry, 3rd ed., John Wiley and sons, New York, p329.

Omolayo, D. and Tope, F. J. (2014). 2D Electrical Imaging Surveys for Leachate Plume Migration at an Old Dump Site in Ibadan South Western Nigeria: A Case Study. *International Journal of Geophysics*, *2014*, p90-92.

Onwuka, S. U., Onuoha, D. C. and Okoye, C. O. (2014).Comparative Analysis of the Soil Geotechnical Characteristics of the Failed and Unfailed Sections of the Onitsha-Enugu Expressway, Southeastern Nigeria. *Journal of Environment and Earth Science*, *4*(16): 125-133.

Rosqvist, H., Dahlin, T., Fourie, A., Röhrs, L., Bengtsson, A. and Larsson, M. (2003).Mapping of leachate plumes at two landfill sites in South Africa using geoelectrical imaging techniques.In *Proceedings Sardinia*.

Sarala T. D. and Uma M. T. (2013). Metal Pollution Assessment in Ground Water: Bull. Env.Pharmacol. *Life Sci*, 2: 122-129.

Singh, P. K., Verma, P., Tiwari, A. K., Sharma, S. and Purty, P. (2015) Review of Various Contamination Index Approaches to Evaluate Groundwater Quality with Geographic Information System (GIS), p 67-83.

Singh, P. K., Tiwari, A. K., Panigarhy, B. P. and Mahato, M. K. (2013). Water quality indices used for water resources vulnerability assessment using GIS technique: a review. *International Journal Earth Science and Engineering*, *6*(6-1) 1594-1600.

Tijani, M. N., Okunlola, O. A. and Abimbola, A. F. (2006). Lithogenic concentrations of trace metals in soils and saprolites over crystalline basement rocks: A case study from SW Nigeria. *Journal of African Earth Sciences*, *46*(5): 427-438.

Unuevho, C., Onuoha, K.M., and A Ikali Y.B.(2012). Direct current resistivitymethods for groundwater prospecting in hardrock terrains: a viable approach to providing sustainable potable water. Centre for Human Settlements and Urban Development Journal, p1-16.

WHO (2011). *Guidelines for Drinking Water Quality (4th Edition)* World Health Organisation, Geneva.